Effects of Oscillatory Activity on Coherence Patterns in the Cerebellar Cortex

Carla Paz Arasanz

A Thesis

In

The Department

of

Exercise Science

Presented in Partial Fulfillment of the Requirements
for the Degree of Masters of Science (Exercise Science) at
Concordia University
Montreal, Quebec, Canada

December 2008

Your file Votre référence
ISBN: 978-0-494-63237-6
Our file Notre référence
ISBN: 978-0-494-63237-6

ABSTRACT

Effects of Oscillatory Activity on Coherence Patterns in the Cerebellar Cortex

Carla Paz Arasanz

The cerebellum is getting more recognized as a rhythm generator, producing oscillations in different frequency bands. While the cerebellum has been associated with motor control, sensory perception, and cognition, the functional role of the granule cell layer oscillations is still elusive. Using awake, unrestrained rats, oscillations were recorded with multiple electrodes in the granule cell layer of posterior lobe of the cerebellar cortex. The purpose of this study was to investigate the effect of oscillations on pattern activity in the granule cell layer. In this study we show that cerebellar oscillations influence the synchrony of local field potential activity across the cerebellar cortex. These oscillations in the frequency range of 6-11 Hz were found to synchronize patterns of local field potentials organized along the coronal plane of the cerebellar cortex. Cerebellar oscillations of the granule cell layer synchronize local field potentials and are integral to the intrinsic circuitry of the cerebellum and play a functional role in spatially organizing cerebellar networks.

ACKNOWLEGDMENTS

This thesis could not have been written without the help of Dr. Richard Courtemanche who not only served as my supervisor but also taught me how to research independently and encouraged me to seek my own truth. I would like to thank Dr. Courtemanche for his time and patience and the endless hours put towards helping me throughout my Masters program. Thank you for helping me to think outside the 'black box'.

I would also like to thank my parents for believing in me and giving me the confidence to believe in myself. My academic career would have been short lived without your support. A special thanks to Domenico Romano and his family for being there during my frustration and helping me stay focused. My 'book' is complete.

Table of Contents

List of Figures

List of Tables

CHAPTER 1:

THEORETICAL CONTEXT

The brain is dynamic and engaged in oscillatory activity. Hans Berger (1873-1941) was the first scientist to discover brain rhythms (Buzsaki, 2006). He performed a number of experiments on himself, his son, and neurological patients using a string galvanometer which recorded electrical activity from the scalp. Hans Berger also was the first to categorize different brain rhythms using different frequency bands. He identified 5 major frequency bands: delta (0-3 Hz), theta (4-7 Hz), alpha (8-12 Hz), beta (13-30 Hz) and gamma (30-200 Hz).

Since Hans Berger's discovery, electroencephalography (EEG) and other electrophysiological techniques have become important tools for the study of brain functions. The signals measured by these techniques reflect the cooperative action of neurons. For example, local field potentials (LFPs) are simultaneous and periodic fluctuations in the membrane potential of a local population of neurons (Mackay, 1998) and while EEG is measured on the scalp, LFPs are measured from inside the brain. These signals can produce brain rhythms, or oscillations, which are due to synchronization of neural activity following a particular temporal pattern. A postulated role for these oscillations is to enable neural synchronization of spatially segregated neurons (Uhlhass et al. 2008). In particular, in the cerebellar cortex of the awake monkey, an interesting phenomenon appears, with oscillations appearing in the granule cell layer when an animal is immobile and attentive; when movement occurs, oscillations cease and LFPs

desynchronize (Pellerin and Lamarre, 1997). This is shown on Fig. 1. One interesting role of these oscillations would be to serve as a system-binding mechanism, facilitating the temporal coordination within systems of the central nervous system (Gray, 1994).

In the quiet, still rat synchronous oscillations occur between theta and beta bands at 5-20 Hz in the Crus II of the cerebellum and the primary somatosensory cortex (SI) (O'Connor et al. 2002). Synchronization of oscillatory activity has also been found in SI, MI, and the cerebellum (Courtemanche and Lamarre, 2005), more strongly between the paramedian lobule (PM) and SI in monkeys during active and passive expectancy tasks when the monkeys were immobile. In the primate PM granule layer, oscillations occurred at 10-25 Hz, and synchrony was most coherent between PM-SI when compared to PM-MI oscillations during the same tasks. PM-SI synchronization during the active condition may characterize cerebro-cerebellar communication, possibly serving as a somatosensory binding tool to perform a task. The weaker PM-MI coherence was also found to be less limb-specific, and its non specificity for movement parameters may indicate a more general type of information being communicated between the two structures (Courtemanche and Lamarre, 2005). Thus, these studies confirm a potential role for oscillatory activity in synchronizing two distant areas for putative information processing, particularly, here, in the case of cerebro-cerebellar relations.

The cerebellum could be viewed as comprising a few rhythm generators (Pellerin and Lamarre, 1997; Courtemanche, 2002; Maex and DeSchutter, 2005). This literature review will first examine the neural circuitry of the cerebellum, establishing known

circuits, and then touch on how its composing cells and signals such as LFPs can become synchronized. The purpose of this thesis is to probe how the synchrony of cerebellar oscillations is organized.

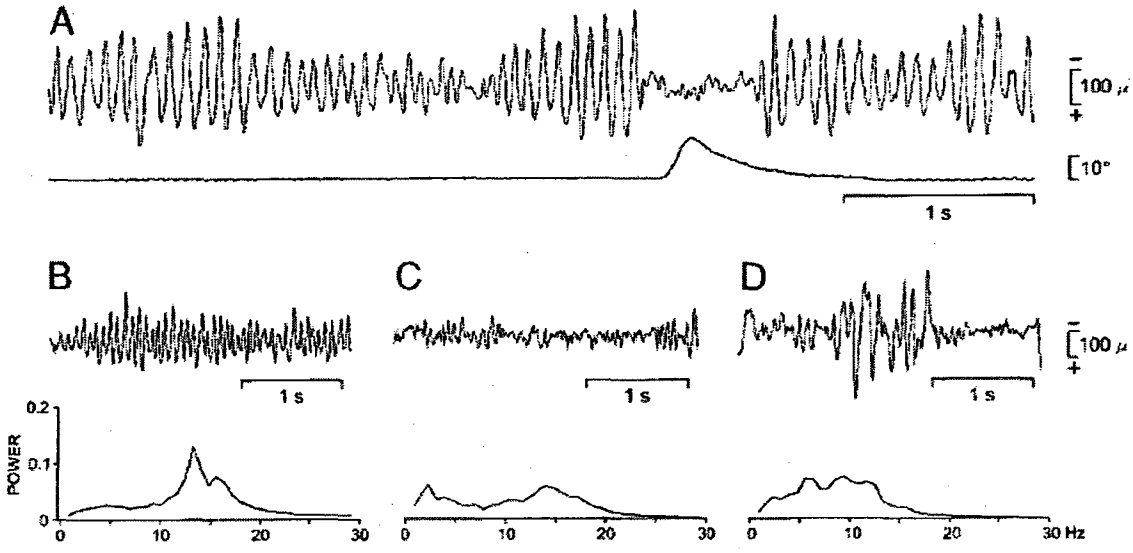

Figure 1. An example of cerebellar modulation of LFP oscillations during monkey elbow flexion (from Pellerin and Lamarre, 1997). A: depicts how oscillations stop at movement onset. B-D illustrate the Power Spectra and LFPs oscillation activity during immobile states of B: quiet wakefulness, C: intense arousal, D: drowsiness.

1.0 The circuitry of the cerebellum

The cerebellar cortex is composed of three distinct layers. Cerebellar granule cells pertain to the granule cell layer (GCL) of the cerebellum; the innermost layer of the cerebellar cortex, after the outer molecular layer and the middle Purkinje cell layer. Granule cells are the most numerous cells in the brain, with about 5×10^{10} granule cells in the cerebellum alone (Llinas, Walton, Lang, 1990). Granule cells are excitatory, exciting all other cell types in the cerebellar cortex (Ito, 1984). Axons of the excitatory granule cells go up the layers, ultimately forming parallel fibers; the ascending axons and the parallel fibers form many synaptic connections with Purkinje cells. Parallel fibers run along the transverse axis, perpendicular to inhibitory pathways, which run sagittally (Ito, 1984).

There are two classical excitatory afferent systems that project to the cerebellar cortex: the mossy fiber and climbing fiber systems. These two systems are anatomically different. Mossy fibers run primarily sagittally and originate from (1) central nervous system regions (via pontine nuclei), and (2) the spinal cord (via spinocerebellar afference). Mossy fibers project to the cerebellar cortex where they synapse on granule cells (Buzsaki, 2006) and also innervate the deep cerebellar nuclei (DCN). The parallel fibers of the granule cells activate wide array of Purkinje cells. This activation is soon inhibited by basket and stellate interneurons that run parallel to Purkinje cells (Llinas, Walton, Lang, 1990). While such inhibition is taking place in the Purkinje cell layer, mossy and parallel fibers activate Golgi cells that are in the granule cell layer. Here,

Golgi cells inhibit granule cells to prevent further activity in parallel fibers. This inhibition is a feedback system that sets the threshold for granule cell firing (See Fig. 2).

Climbing fibers on the other hand originate from strictly one source, the inferior olive, and branch into fibers once inside the cerebellar cortex. Here they bypass granule cells and synapse directly onto one Purkinje cell each (Llinas, Walton, Lang, 1990). Complex spikes are generated by climbing fibers and fire simultaneously along Purkinje cells aligned parasagittally in the cerebral cortex (Lang, Welsh, Llinas, 1999). This is due to the branching pattern of the olivocerebellar axons, which run in straight narrow lines along the rostrocaudal axis from the brainstem to the cerebellar cortex. Climbing fibers also activate inhibitory interneurons and Golgi cells; they therefore inhibit the input coming from the mossy fibers and dominate Purkinje cells when they fire.

While the climbing fiber system is organized to produce synchronous activation of Purkinje cells organized parasagittally, parallel fibers are oriented mediolaterally. The organizational array of parallel fibers that cross perpendicular to Purkinje cells are believed to form a structure that may act as delay lines for temporal processing of accurate time intervals (Braitenberg, 1967). Theoretically, each mossy fiber that approaches the granule cells will send out the same signal to hundreds of Purkinje cells via one row of parallel fibers. This information is distributed in a strict temporal sequence by a traveling wave of parallel fiber activity, the rate and timing which are determined by the 0.5 m/s conducting velocity of the parallel fiber. The proposed time-sensitive system, or clock, could translate time into distance and be ideal for short intervals and rapid

voluntary movements. However, this 'clock' idea is flawed because at their slow conducting speed, parallel fibers would need to be 50 mm long to produce delays of 100 ms (Heck and Sultan, 2002). Electrophysiological studies have also revealed that single parallel fibers have a weak effect on postsynaptic firing probability; therefore they might not be the major source of excitatory input to Purkinje cells (Heck and Sultan, 2002).

How the mossy fiber and the climbing fiber system of the cerebellum produce functionally meaningful cerebellar output is still not resolved. This next section takes a look at cerebellar oscillations and how they modulate neural behavior.

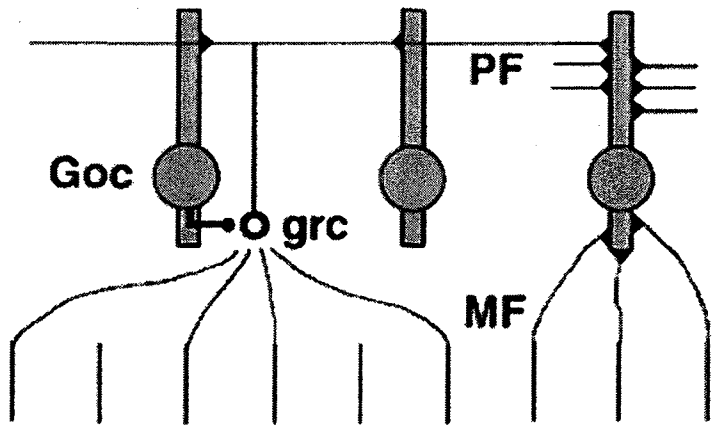

Figure 2. Golgi cell- granular cell inhibition feedback circuit. Golgi cells (Goc) inhibit granule cells (grc) to regulate excitation of parallel fibers (PF). Afferent input is received via mossy fibers (MF). Illustration from Volny-Luraghi et al. (2002).

1.1 The Role of Cerebellar Oscillations

Cerebellar oscillations have been found to occur in the climbing fiber input to the cerebellum (Welsh et al., 1995), the granule cell layer (Hartmann and Bower, 1998; O'Connor, 2002; Courtemanche and Lamarre 2005), molecular layer (Middleton et al. 2008), and the Purkinje cells recurrent collaterals (de Solages et al., 2008). These oscillations have been found in various frequencies across the spectrum, from theta rhythms (Hartmann and Bower, 1998) to very fast oscillations (Middleton et al., 2008; de Solages et al., 2008). What would be interesting to know is which of these cerebellar oscillations serve behaviorally relevant functions and which merely reflect an echo of reverberating activity within the cerebellar cortex (De Zeeuw et al. 2008). At the same time, the significance of these oscillations in the cerebellar network organization has to be worked out.

Very fast oscillations (VFOs) were observed by in-vitro cerebellar recordings (Middleton et al., 2008). These VFOs resemble the spatiotemporal organization of olivary generated oscillations. Gamma rhythms (30-80 Hz) and VFOs (80-160 Hz) have been found in cerebellar cortical areas when pharmacologically induced by nicotine (Middleton et al., 2008) VFOs, as previously mentioned, are dependent on an inhibitory mechanism that runs parasagittally across crus I and II while gamma oscillations are oriented transversely (Middleton et al., 2008; De Zeeuw et al., 2008) Lateral gamma rhythms have been observed in other brain regions, such as the hippocampus and neocortex; and may also be generated by networks of inhibitory neurons (Whittington et al., 1995). Besides the cerebellar cortex producing rhythms within the same frequency band as neocortical structures, the phenomenon of synchronization across these structures

at such high frequencies is unknown, making VFOs' relevance questionable. This however is not the case for beta oscillations detected in monkeys (Courtemanche and Lamarre, 2005), where cortical oscillations within this band have been found to synchronize with oscillations in the primary somatosensory cortex during active expectancy.

Cerebellar oscillations in the theta and beta band are unique to the granule cell layer (GCL). The frequency of the LFPs is modulated according to level of vigilance, and stop when movement is initiated. In an electrophysiological study using primates, Pellerin and Lamarre (1997) observed the longest oscillations during elbow flexion task when the subjects were attentive and in a task focused state. Oscillations also increased in size just before movement onset. The "spindle" shaped activity of these oscillations is suggestive of the primates' movement preparation before the stimulus occurs. But what generates these GCL oscillations? And how may they influence GCL LFP synchrony?

In rodents, a similar GCL oscillatory activity has been recorded (Hartmann and Bower 1998; O'Connor, 2002). More specifically, Hartmann and Bower (1998) as well as O'Connor et al. (2002) looked at whether the frequency produced during whisking was coherent with GCL oscillations in crus IIa of unrestrained rats. Hartmann and Bower (1998) were solely interested the oscillatory activity in the cerebellar hemispheres during immobility. They found that oscillations occurred at 7-8 Hz and ceased spontaneously, without any sensory input or movement. In relation to when the animals whisked, they found that GCL LFPs during whisking was different from the oscillations observed when

the animal was still. Hartmann and Bower (1998) however did not quantify a whisking frequency. O'Connor and colleagues (2002) on the other hand determined a whisking frequency at 7-8 Hz using three EMG electrodes placed in the right myostatial pad of the rats. Additionally, this study looked at the coherence between vibrissae areas in SI and the cerebellum. Internal coherence was found to between these two structures for 30-40% of free whisking. SI and crus IIa of the cerebellum shared a frequency of 8-9 Hz in these sensory sensitive areas. However, the power of these oscillations decreased in the cerebellum during whisking. The data implies that although whisking and signaling between SI and the cerebellum share the same frequency band, this internal signaling is incoherent with whisking and therefore must serve another behaviourally relevant purpose. The possibility still remains that the GCL circuits could obey different rules for oscillation; however, it appears that a pure afferent input is not driving the activity.

Cerebellar GCL LFPs have been shown to be synchronized along parasagittal planes (Courtemanche, 1999). These GCL LFPs were found in the cerebellar cortex of primates at rest, in between trials where a lever was to be pressed 1.5 s after a sound stimulus to receive a reward (active expectancy). They were also seen in trials where no action was taken following a sound stimulus (passive expectancy), and in conditions where the subjects were simply at rest. The synchrony between GCL LFPs did not differ between task conditions; however during active conditions, synchrony was also found transversely along the coronal plane. During periods of oscillations, LFP synchrony was strongest in both sagittal and coronal directions, compared to when oscillations where not as present. The expanding of LFP synchrony into the coronal direction during task

execution is particularly interesting as it may be caused by an internal circuit in the GCL that produces oscillations within the 10-50 Hz band (Courtemanche, 1999).

Granule cell firing is controlled by inhibitory Golgi cells (Marr, 1969; Ito, 1984). This unique property that the inhibitory and excitatory neurons share causes a pure feedback circuit to occur, synchronizing the Golgi and granular cell populations into a rhythm (Maex and De Schutter, 1998). The internal circuit is known as the granule cell-Golgi cell circuit. According to the computational model devised by Maex and De Schutter (1998), the synchronous rhythm occurs at a frequency ranging from 10 to 40 Hz, and is dependent on the firing rate of mossy fibers. Under strong mossy fiber input, Golgi cells fire rhythmically and synchronized with granule cell along the parallel fiber axis. This synchrony lasts large distances of over 2 mm strictly along the transverse axis, implying an integral role for common parallel fibers and negative feedback of Golgi to granule cells excitation, in such rhythm genesis. To test this model, Vos et al (1999) used multielectrode extracellular recordings to see whether Golgi cells affect the timing of granule cells spikes. They recorded pairs of Golgi cells positioned either along the transverse axis, that share common parallel fiber input, or sagittal axis (no common input) of anesthetized rat cerebella. Results suggested that Golgi cells that are aligned transversely are synchronized, whereas those recorded along the parasagittal axis were not synchronized. Therefore, Golgi cells may aid in the control of the timing of granule cell firing, however; it is the common parallel fiber excitation which contributes to coherence in granular cell spikes. It is possible that the oscillations produced by the

Golgi cell-granule cell circuit, may also have a role in the synchrony of GCL LFPs, since this circuit can be modulated spatially via parallel fiber afferent input.

1.2 Synchrony in the Cerebellar Cortex: Purkinje Cells

Synchronization of neurons across large systems has been found to increase the salience of signals, and to facilitate their propagation across sparsely connected networks (Uhlhass et al. 2008). Synchrony may also complement binding mechanisms of an individual structure, such as the cerebellum. Purkinje cells of the cerebellum have been reported to synchronize in a spatial organization. Although rhythmic firing is not always present in complex spikes (Keating and Thach, 1995; Yarom and Cohen, 2002), synchronous complex spikes were observed parasagittally at a 10 Hz frequency during an *in vivo* study in rats (Lang et al., 1999). This provides evidence that the olivocerebellar system is capable of generating organized, rhythmic activity (Lang et al. 1999).

Other studies that have investigated the population dynamics of Purkinje cell activity (Shin and De Schutter, 2006; de Solages et al 2008) have found millisecond synchrony between neighboring Purkinje cells that fired at fast rhythms of around 200 Hz. Firing of single Purkinje cell units did not display such rhythmicity, but the collective population generated a high-frequency oscillation of over 100 Hz. These very high frequency oscillations (VHFOs) are strongest in the Purkinje cell layer and molecular layer of the cerebellar cortex and appear to be generated in these layers as well. Found at 120-240 Hz in anesthetized and awake rats, the oscillations likely serve as the promoter for synchrony of the Purkinje cells; however are independent of the firing rate

of individual cells. Interestingly, synchrony in the cerebellar cortex was patch-like, with coherence in both the parasagittal and transverse direction over distances of 10 Purkinje cells. Thus, de Solages et al. (2008) and her colleagues conclude that Purkinje cell activity had no directional preference in the cerebellar cortex and its recurrent collaterals may temporally organize cerebellar output.

Heck, and his collaborators Thach and Keating (2007), used microelectrodes to record pairs of Purkinje cell simple spikes, in crus II and the paramedian lobule, that fired either along a shared parallel fiber input (across the transverse axis) or perpendicular to these excitatory neuronal processes (parasagittal axis). The authors trained rats for a task that involved reaching and grasping a food pellet. In electrodes placed sagittally, no time correlation was found between simple spikes. However, in electrodes that ran transversely the authors found two types of temporally correlated simple spike activity; a weak delayed temporal correlation, and a strong synchronous correlation with zero lag. For the former, the delay of the second simple spike pair matched the estimated parallel fiber conduction velocity (0.5 m/s) that Braitenberg proposed (1967), however the delayed correlation was rarely observed, only occurred for short distances, and was poorly time-locked to movement. For the latter, simple spike correlations for the Purkinje pairs were simultaneous, firing with zero delay. This synchrony occurred during reaching and grasping movements, and where time locked to the touch of the food pellet (reward). The electrodes placed along the parallel fibers recorded simple spikes that fired synchronously. However, their behaviour related firing rates were variable and not temporally correlated. As a result, the authors could not conclude that parallel fiber input

solely shape the response property of Purkinje cells; and suggest that mossy fibers that branch and provide common input to granular cells, are what provide synchronous excitatory input to the Purkinje cells. Thus, Heck, Thach, and Keating (2007) propose the mossy fiber-granule cell- Purkinje cell circuit, and not just the parallel fibers, that is responsible for the synchrony found between simple spikes along the transverse axis of the cerebellar cortex.

The mossy fiber afferent system is governed by spontaneous and synchronous activity. Could such synchrony be serving a functional purpose? How cerebellar oscillations influence pattern activity in the GCL is integral to this study.

CHAPTER 2:

RATIONALE AND OBJECTIVE

The purpose of this study is to find oscillatory activity in the granule cell layer of the cerebellum and identify their effect on network activity in the cerebellar cortex. Oscillations have been found to occur during quiet wakefulness, when an animal is still and attentive (Hartmann and Bower; O'Conner et al. 2002; Courtemanche et al. 2002; Pellerin and Lamarre, 1997). Using multi-cellular and LFP neurophysiological recordings in rodents, LFP oscillations were recorded from 3-7 electrodes in the granular cell layer of lateral Crus II and paramedian lobule of the cerebellar cortex. These brain areas were selected for their reported association with rhythmic oscillatory activity (Pellerin and Lamarre, 1997). The objective of this is to evaluate the influence of GCL cerebellar oscillations on GCL LFPs synchrony. Coherence test between each electrode will be used to compare the activity of LFPs from one recording site to the other during oscillatory periods and non oscillatory periods. The intention of this test is to establish if there is synchrony between the LFP activity recorded from each electrode. Synchrony is important because it would reveal the basic patterns of activity in the GCL. Synchrony implies that the pattern of neural activity is spontaneous but not random. If oscillations influence synchronous activity across the GCL, then they may participate in activating Purkinje cells to travel to the nuclei. The rationale of evaluating the oscillatory role on LFP synchrony in the GCL is ultimately to identify whether oscillations are intrinsic and influential in cerebellar circuitry.

CHAPTER 3:

HYPOTHESIS

We postulate that cerebellar oscillations influence the synchrony of granule cell layer LFPs. Serving an intrinsic purpose, we hypothesize that coherence will be modulated in the following manner:

1. Oscillations and LFP Synchrony:

   During the occurrence of oscillations, we propose that synchronous activity of the granule cell layer local field potentials will be recorded from pairs of electrodes.

2. Orientation and Synchrony:

   The orientation of how the electrodes are arranged may affect the pattern of GCL synchrony. We hypothesize that electrodes arranged along the transverse axis will record oscillations that cohere more so than those arranged along the sagittal plane.

3. Electrode and Synchrony:

   Not all electrodes (channels) will be used to detect oscillatory periods, (i.e. be a 'detected' electrode). Since oscillations will only be identified on strong GCL oscillations i.e. electrodes with known GCL properties, we speculate that channel comparisons that share a 'detected' electrode will be more coherent than comparisons with no 'detected' electrodes.

CHAPTER 4:

METHODOLOGY

4.0 Subjects and Apparatus:

Three naive Sprague-Dawley male rats, approximately three months of age at the start of the experiment, were used for this study. Rats were kept in a temperature-controlled room, under a 12/12 hour light-dark cycle. The apparatus consisted of one standard operant box with dimensions of approximately 24 x 31 x 31 cm and a grid floor composed of stainless steel rods. Side and top panels were made of metal and clear Plexiglas. Each rat was equipped with a recording chamber (headstage) that encompassed a reference electrode, a ground, and independently moveable tungsten uni-polar microelectrodes (0.5 – 4 MΩ), that could record multi-cellular activity and LFPs (See Fig. 3). Not all electrodes were used for analysis. Three electrodes were selected from each rat, based on the quality of their recording.

4.1 Headstage:

Electrodes were placed in a multi-electrode carrier known as a headstage. Electrode arrangements within each headstage differed between rats to investigate the effect of different orientations on LFP synchrony. Rat 1 had seven electrodes. Electrodes were either paired or placed alone into one of four tubes (needles) arranged in a square formation of 2mm by 2mm. Not all electrodes were used for analysis. For Rat 1, electrodes 4 and 5 were damaged and gave poor signal. Electrodes 1, 3 and 6 recorded the best signals; 1 and 6 sharing a same needle and 3 in a needle situated diagonally from 1

and 6. Rat 2 had five electrodes, 1 and 2 sharing a needle placed medially, along the coronal axis, from electrodes 3, 4 and 5. Electrodes 1, 2, and 3 were used for analysis due to poor signal recorded from electrodes 4 and 5. Rat 3 had three electrodes that shared the same needle. Figure 4 illustrates the electrode arrangements for all three rats.

Figure 3. Rat headstage. A multiple electrode carrier (headstage) was used to record LFP activity in the right hemisphere of the rat cerebellum. Each headstage had between 3-7 independently moveable tungsten electrodes.

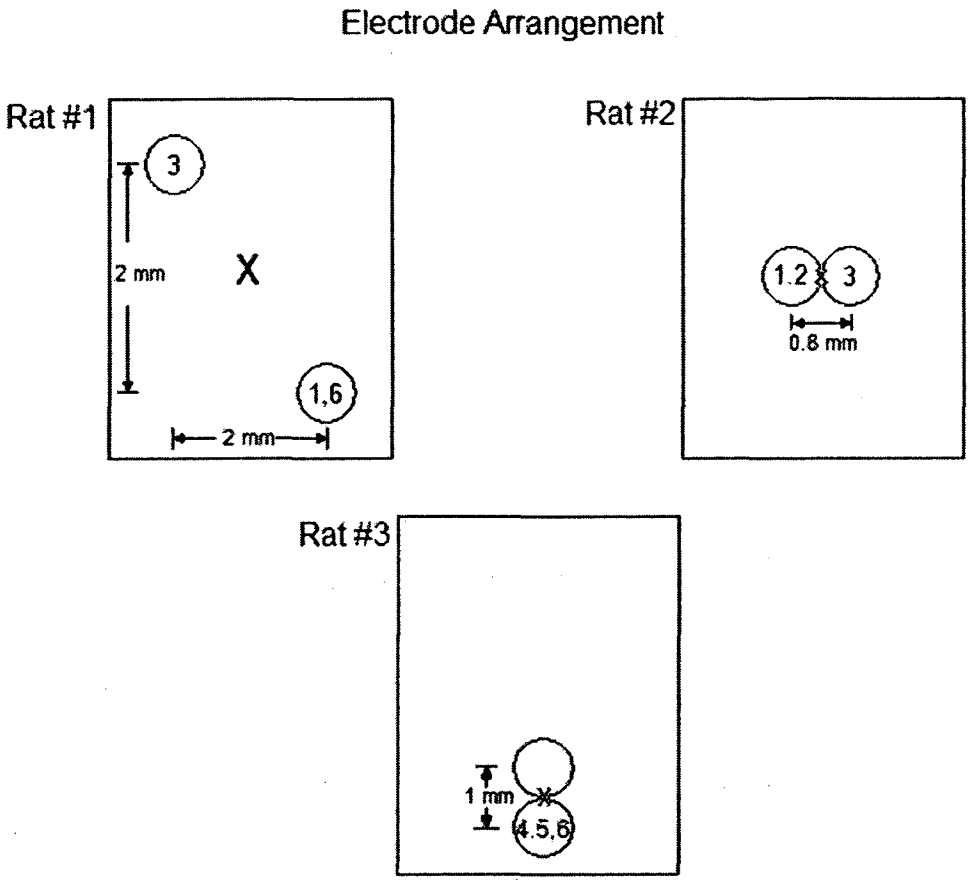

Figure 4. Electrode arrangement of each rat. Numbers indicate the electrode number used for analysis. Circles represent the needles that encompass the electrodes. Arrows represent the distance of the needles. X represents the position of the reference electrode on the headstage tip.

4.2 Surgery:

All procedures have been approved by Concordia Animal Care Committee. About one week prior to testing, subjects were anesthetized with ketamine (100 mg/kg), xylazine (50 mg/kg) and atropine (80 mg/kg), by means of intramuscular injections. A booster shot of extra ketamine at 20% of its initial dose was administered only if it was required during surgery to prevent the rat from waking. Body temperature was maintained at 36 °C +/- 1 °C using a heated pad and a rectal temperature probe for the

length of the surgery. To keep the rat hydrated, a body-temperature saline solution was injected at 5 cc subcutaneously every 30 minutes.

After being anesthetized, the subjects' head were fixed using a stereotaxic apparatus and layers of derma and occipital muscles were cut to allow for sufficient access to the subjects' skull. Six screws were then drilled into the skull to support a headstage containing 3-7 tungsten electrodes and a reference. The electrodes and reference were lowered into the right hemisphere of the cerebellum, aimed for lateral crus II and paramedian lobule (PM). Target was made using stereotaxic coordinates based on a rat brain atlas (Paxinos and Watson, 1986).Before the headstage was properly placed, mineral oil was used to coat the electrodes and prevent blood from trapping inside the tubing that housed the electrodes. Dental acrylic was smoothed around the screws to fix and secure the head stage. Lastly, skin was sutured to close all open wounds around the head of the subject rat and a dose of buprenorphine (60 mg/ kg) was administered after the surgery for pain relief once the rats had waken.

4.3 Recording and Data Analysis:

During a recording session, single- and multi-unit activity (600-6000 Hz) and LFPs (1-125 and 1-475 Hz) were recorded with the appropriate filter settings. One second windows were used to analyze oscillatory activity and coherence during recordings. Windows were analysed for two different behaviors; when rats were immobile and oscillating, immobile and not oscillating. NeuroExplorer and MATLAB were used throughout analysis for these two variables:

- Oscillations and Rhythmicity:

  Raw data of LFP was first filtered for valid recording period - periods in which no artifacts i.e. scratching, sniffing, grooming, were present. Each rat had multiple recording sessions. Three recording sessions were selected for each rat based on the number of valid recording periods it contained, as well as whether or not the sessions contained oscillatory periods. Spectral power density is a tool used to detect the modulation of oscillatory activity. Spectral power densities were used to evaluate the rhythmicity of the local field potentials during neural recording sessions. Rhythmicity was quantified in the 6-11 Hz range (O'Connor et al. 2002). After assessing recording sessions, the best three sessions underwent 'oscillatory detection' using algorithm that detected the relative power of the 6-11 Hz band vs. the adjacent bands, in Matlab. This algorithm detected oscillatory rhythmicity within the range of 6-11 Hz, and singled out the time periods during which this occurred. LFPs were detected as 'oscillatory' if they withstood a period of 1 s or longer. By virtue of our test, LFPs that were not detected as 'oscillatory' were used as controls (non-oscillatory periods).

- Synchronization and Coherence:

  One advantage of recording from multiple electrodes is the ability to detect patterns of how LFPs are temporally related. After oscillations were detected on a strong GCL channel, the top three electrodes with the greatest number of detected oscillatory periods underwent another algorithm in Matlab, which was used to assess coherence between electrodes during the 'detected oscillatory' periods and the non-oscillatory

control periods. Coherence can be used to examine the relationship between two signals. The relationship is a measure of the similarity between both signals, as a function of frequency. Values of coherence (C) will always satisfy $0 \leq (C) \geq 1$. Coherence is equal to one when two signals are completely phase locked. For this study, coherence was defined as the mean coherence between 6-11 Hz, (see Fig 5). Coherence in this band was compared across all channels (i.e. channel 1x2, 1x3, 2x3) for each rat. For coherence analysis, time window consisted of 1 s periods.

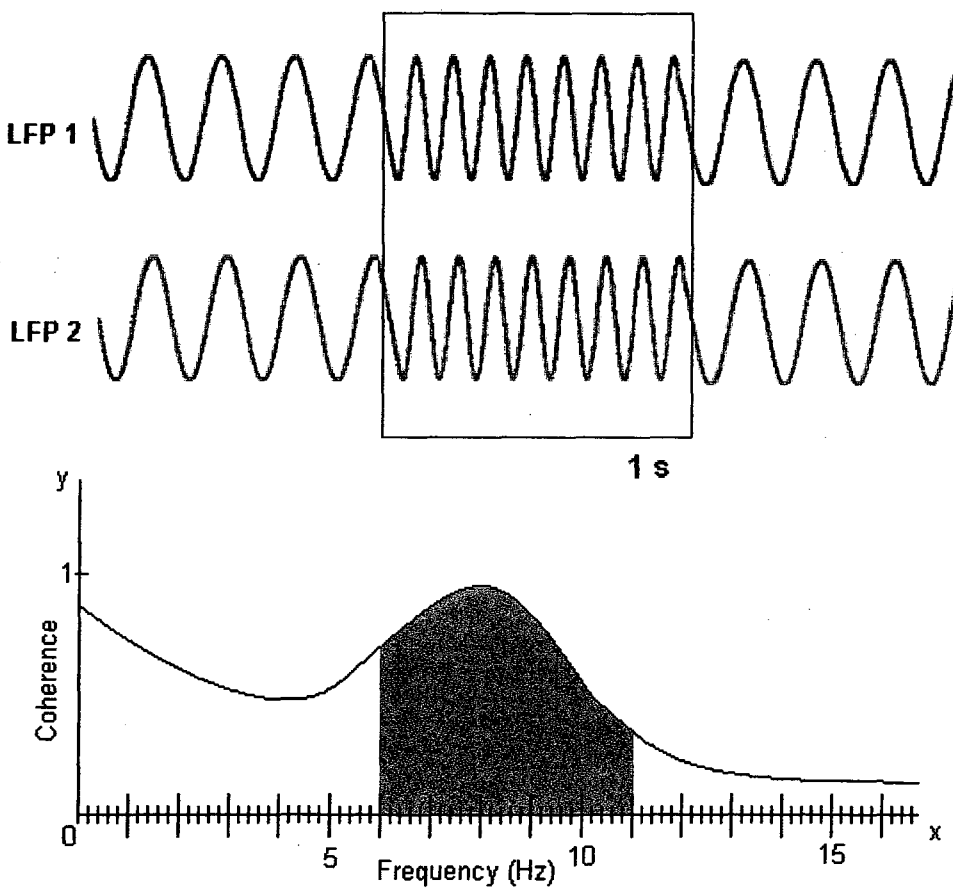

Figure 5. Identifying coherence as a mean between 6-11 Hz. The LFP signals from two recorded electrodes were compared to calculate their phase relationship. Coherence analysis consisted of 1 s time windows. Coherence (y-axis) was measured as a function of frequency (x-axis). Coherence was defined as the mean coherence between 6-11 Hz.

4.4 Histology:

At the conclusion of the recordings selected electrolytic lesions were made to mark the position of the electrodes. The animals were euthanized using a CO_2 gas chamber and the brain was extracted and placed in a 10 % formalin solution. Prior to histology, the intact brain was placed in a 20 % sucrose-formalin solution until the brain sank. To locate and verify recording sites, standard histology using cresyl violet was performed on 50 μm frozen sagittal slices of the cerebellum.

4.5 Statistics:

Statistics consisted of one way and multi-factorial ANOVAs.

- Coherence vs. Periods:

  To evaluate the effect of oscillatory periods versus non-oscillatory periods on coherence across rats, a one-way ANOVA was performed. Coherence was the dependant variable and Periods was the independent- grouping variable (oscillatory, non-oscillatory controls). However because the dependant variable 'Coherence' did not fall into a normal distribution, Kruskal-Wallis non-parametric ANOVA test was performed instead.

- Coherence vs. Rat:

  Coherence was also tested for each rat independently. Here, Kruskal-Wallis non-parametric ANOVA test was used to evaluate the main effect of Rat (Rat 1, 2, 3) by Period (oscillatory, non-oscillatory controls) on Coherence (mean coherence).

- Coherence vs. Orientation:

  Orientation of electrode arrangement was another variable used for analysis. The Kruskal-Wallis non-parametric ANOVA test was used to identify the main effect of Orientation (diagonal, coronal, same needle) by Rat (Rat 1, 2, 3) by Period (oscillatory, non-oscillatory controls) on Coherence (mean coherence).

- Coherence vs. Detected electrode:

  A test to see whether the electrode used for 'oscillation detection' showed statistical significance over non-detected electrodes was performed using the Kruskal-Wallis non-parametric ANOVA test. This test identified the main affect of Detected Electrode (detected, non-detected) by Rat (Rat 1, 2, 3) by Period (oscillatory, non-oscillatory controls) on Coherence (mean coherence).

CHAPTER 5:

RESULTS

5.0 Database

Three recording sessions were used per rat for analysis. For each rat, three electrodes were used to record LFP oscillations. For many periods during the recordings, LFPs were oscillatory within a 6-11 Hz range, but this phenomenon would be waxing and waning. Electrodes of each rat were paired to determine coherence between channels. Comparisons were made for coherence during oscillatory and non-oscillatory periods. During each recording session, oscillatory periods were determined for an electrode in the GCL; for these periods, the coherence within the 6-11 Hz range between two LFPs was calculated; inversely, for other windows, control periods were classified as 'non-oscillatory', and the 6-11 Hz coherence was also calculated for these samples. Table 1 lists the database parameters for each rat.

	Rat 1	Rat 2	Rat 3	Total
Sessions	3	3	3	9
Electrodes	1,3,6	1,2,3	4,5,6	9
Oscillatory Periods (n)	1716	1143	2676	5 535
Non Oscillatory Controls (n)	9047	6616	7915	23 578
M/L Coordinates for implant (mm)	3	2.5	3	N/A
A/P Coordinates for implant (mm)	12.5	13	13	N/A
Electrode comparisons	1*3 1*6 3*6	1*2 1*3 2*3	4*5 4*6 5*6	9
Site Comparisons	19	9	13	41
Orientation	-Diagonal -Same Needle	-Coronal -Same Needle	-Same Needle	- Coronal -Diagonal -Same Needle
Detected Electrodes	1, 3, 6	3	4	5

Table 1. Database Parameters. Table of the independent variables used for analysis and to create a database of Rat 1, 2, 3. Three analyses for each rat involved: 3 recording sessions, 3 electrodes, and 3 electrode comparisons. The medio/lateral (M/L) and anterior/posterior (A/P) are listed different for each rat, as well as the orientation (Diagonal, Coronal, 'Same Needle' and Detected Electrodes. The total number of oscillatory periods and controls, as well as the number of site of electrode comparisons, also differ between rats.

A total 41 recording sites were used for analysis. Sites varied according to rat, session, channel comparisons and electrode depth (See Table 2). For each recording site, the Kruskal-Wallis ANOVA test was used to evaluate the influence of non-oscillatory and oscillatory periods on coherence. This test was necessary due to a distribution of values that were not normal. Therefore, the Kruskal-Wallis ANOVA test compares medians, and not means. The comparisons in Table 2 are merely a description of all the comparisons taken together. Rat 1 had 19 comparisons between recording sites, Rat 2 had 9, and Rat 3 had 12. Most comparisons show an oscillatory influence on coherence, as indicated by the p values of each recording site. The analyses that follow separate these site comparisons according to rat, orientation, and electrode detection to view the effect of oscillations from each of these standpoints.

Prior to euthanizing the rats, lesions were made at recording sites with the presence of a recorded cell or strong oscillations. Histological localization of lesions revealed that the recording sites of the electrodes fell within the targeted lateral crus II and paramedian lobule of the right cerebellum. Figure 6 shows a recording site of rat 1 in a prepared sagittal cerebellar slice.

Rat	#	I.D	Channels	Df	N	H	P	Median non-oscillatory	Rela-tive	Median oscillatory
	1	1	1*3	1	801	0049245	0.9441	0.350525		0.354493
	2	28	1*3	1	193	4.917824	0.0266	0.268390	<	0.389173
	3	29	1*3	1	150	3.308854	0.0689	0.215757		0.275574
	4	4	1*3	1	494	.4656973	0.4950	0.382780		0.385215
	5	32	1*3	1	591	3.542591	0.0598	0.398211		0.438268
	6	7	1*3	1	729	1.586849	0.2078	0.367988		0.294665
	7	34	1*3	1	617	1.363671	0.2429	0.382074		0.335471
1	8	2	1*6	1	401	.2162281	0.6419	0.484154		0.486624
	9	30	1*6	1	747	.9768909	.3230	0.734057		0.707037
	10	5	1*6	1	1095	5.398737	0.0202	0.870963	<	0.886303
	11	8	1*6	1	1354	5.400802	0.0201	0.816595	>	0.791053
	12	3	3*6	1	401	1.355433	0.2443	0.346321		0.260687
	13	31	3*6	1	151	9830341	0.3215	0.309213		0.319120
	14	41	3*6	1	405	.4643289	0.4956	0.346992		0.333991
	15	40	3*6	1	191	10.38890	0.0013	0.342903	<	0.450924
	16	6	3*6	1	498	3.278992	0.0702	0.388198		0.341673
	17	33	3*6	1	597	.9051422	0.3414	0.417968		0.419577
	18	9	3*6	1	729	.9027281	0.3421	0.406533		0.378711
	19	35	3*6	1	617	.7443020	0.3883	0.419589		0.470133
	20	10	1*2	1	1204	14.17332	0.0002	0.248138	<	0.299940
	21	13	1*2	1	493	1.070031	0.3009	0.398304		0.370429
	22	16	1*2	1	889	11.76751	0.0006	0.296423	<	0.367087
	23	11	1*3	1	1204	198.0870	0.000	0.367354	<	0.683180
2	24	14	1*3	1	493	7.782668	0.0053	0.337025	<	0.460520
	25	17	1*3	1	888	27.64708	0.0000	0.340964	<	0.493599
	26	12	2*3	1	1204	9.106024	0.0025	0.230838	<	0.282001
	27	15	2*3	1	496	21.45197	0.0000	0.713600	>	0.527968
	28	18	2*3	1	888	30.27248	0.0000	0.246654	<	0.367227
	29	19	4*5	1	1014	9.062318	0.0026	0.675808	<	0.750532
	30	36	4*5	1	490	215.3779	0.000	0.676057	<	0.900786
	31	22	4*5	1	1016	9.623940	0.0019	0.538555	<	0.592413
	32	38	4*5	1	330	74.33203	0.0000	0.670984	<	0.893552
	33	25	4*5	1	681	292.5877	0.000	0.653147	<	0.916846
3	34	20	4*6	1	1504	244.3098	0.000	0.344571	<	0.696632
	35	23	4*6	1	1346	85.52149	0.000	0.437985	<	0.583015
	36	26	4*6	1	680	280.6950	0.000	0.591762	<	0.871300
	37	21	5*6	1	1014	.7732810	0.3792	0.472300		0.459608
	38	37	5*6	1	490	145.7803	0.000	0.520187	<	0.838043
	39	24	5*6	1	1002	2.022486	0.1550	0.555761		0.578652
	40	39	5*6	1	337	75.90228	0.0000	0.656613	<	0.897771
	41	27	5*6	1	681	286.0362	0.000	0.665947	<	0.932930

Table 2. Electrode site comparisons. Electrode site comparisons for each rat with their significance (significance if $p < 0.05$) and non-parametric Kruskal-Wallis ANOVA test scores. (#) is the number of comparison site; (I.D) is the identification number of the site; (Channels) are the electrodes used in the comparison; (Df) are the degrees of freedom; (N) is the number of comparison for a particular site; (H) is the score of the Kruskal-Wallis test; (p) is the significance; (Relative) compares the median value of the oscillatory periods to the controls (non-oscillatory) (<,>).

Figure 6. Histological localization of lesions. The prepared cerebellar slices of Rat 1 indicate the recording area of electrode 1. The red arrow head points to the location of the lesion. Lesion of electrode 1 was found lateral 3.40 mm from the midline of the cerebellum.

5.1 Do oscillations influence coherence?

Oscillations in the crus II and PM had an effect on synchrony between recording electrodes in the GCL of the right cerebellum. Oscillations would cease and reappear on paired electrodes simultaneously, creating instances of detectable oscillatory and non-oscillatory periods. When oscillations were present, there was a tendency for LFP to synchronize. This phenomenon is described in Fig. 7A, which displays an example of the LFPs simultaneously recorded between two electrodes. In this example, synchrony was strongest when the rat was quiet and immobile and weakened when oscillations ceased. Fig. 7B illustrates in a spectrogram the coherence found between the two recording electrodes. This spectrogram reveals strong coherence between electrodes in the 6-11 Hz frequency range.

5.2 Coherence during oscillatory periods and non-oscillatory controls

Fig. 8 reveals the global influence of oscillations on LFP coherence, pooled for all rats. Even if we have more observations for non-oscillatory control periods than for oscillatory periods, it is nonetheless apparent that most of the observed oscillatory periods provide higher coherence values with the histogram being shifted to the right. The box and whisker plot in Fig. 8B illustrates the difference between non-oscillatory controls and oscillatory periods. Coherence was greatest among the oscillatory periods compared to the non-oscillatory controls. A non-parametric global analysis using the Kruskal-Wallis ANOVA displayed a significant difference between coherence during non-oscillatory control periods and oscillatory periods $H(1, N= 29105) =1077.445$.

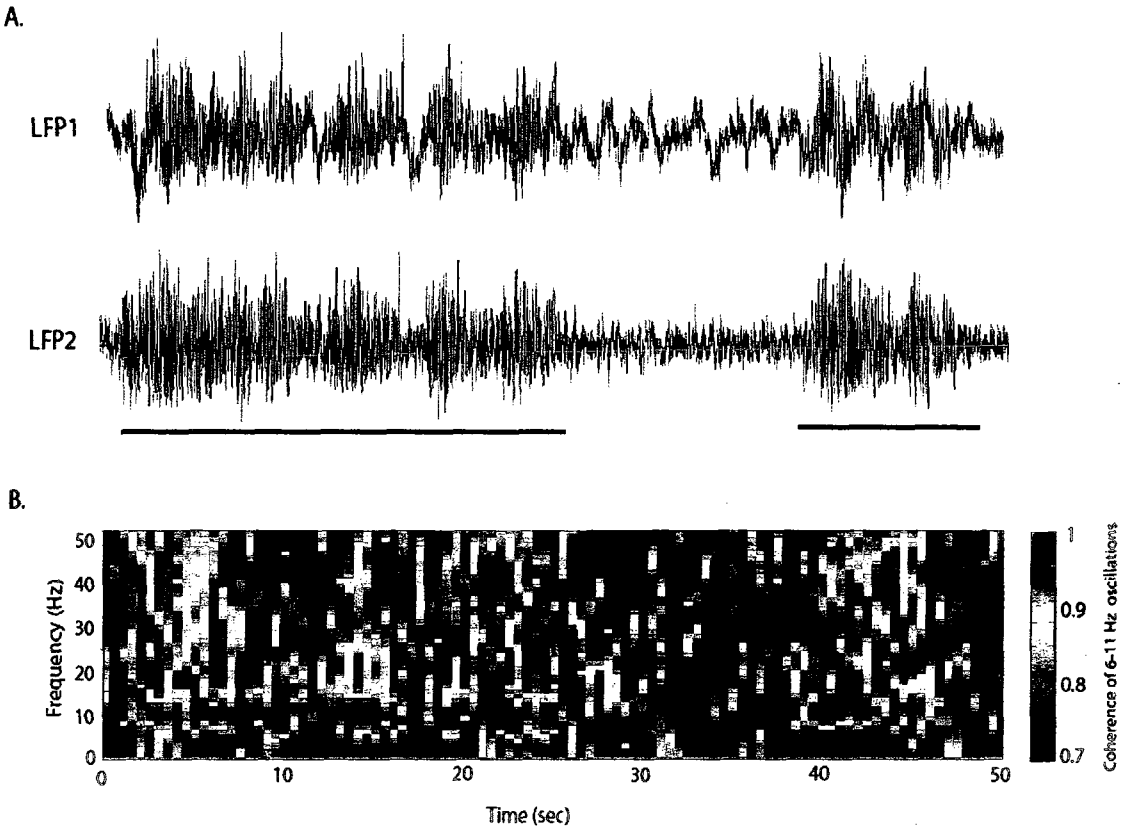

Figure 7. Local Field Potentials recorded simultaneously in the paramedian lobule (PM) of the cerebellum. A: LFPs recorded from two different electrodes in rat 3. Periods of oscillations (6-11 Hz) were observed when the animal was in a quiet and resting state (underlined). B: Spectrogram of coherence between recording electrodes in (A) over a 50 second period. Left y-axis displays the different frequencies present in the recording period, and the right y-axis displays the coherence at each frequency. Note that the coherence between LFPs of each electrode is strongest during periods of oscillations in the 6-11 Hz frequency range.

A.

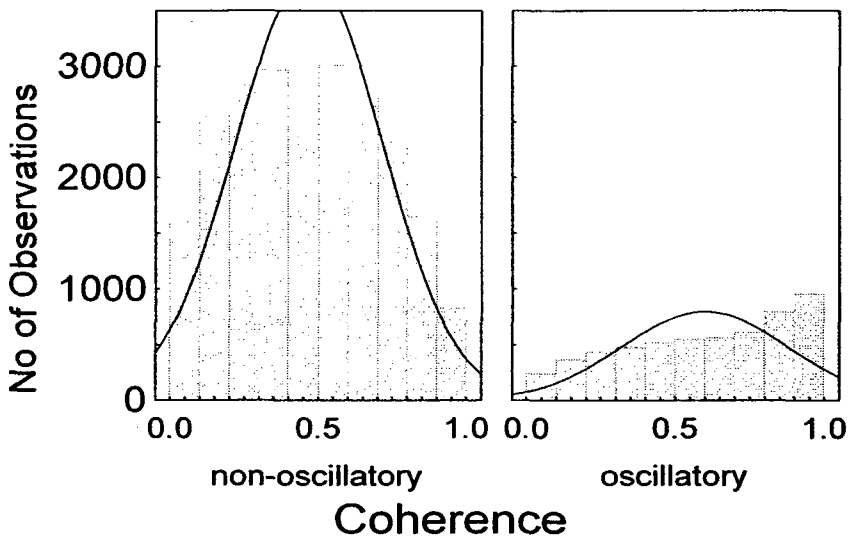

B.

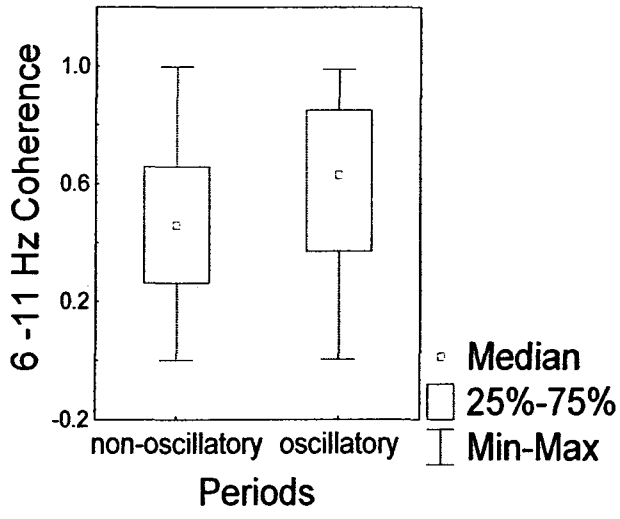

Figure 8. Coherence during non-oscillatory controls and oscillatory periods across all rats. A: Histogram comparing the distribution of the coherence of non-oscillatory controls and oscillatory periods. B: Box and whisker plot of the values for coherence for non-oscillatory (0.552) and oscillatory periods (0.751). This difference was significant at $p < 0.05$ using the Kruskal-Wallis non-parametric ANOVA test.

5.3 Coherence for each rat

The influence of oscillations on LFP synchrony was also analysed on each rat individually to see if the results were consistent throughout. While oscillation frequencies stayed within the same range, coherence across LFPs varied from subject to subject. Fig. 9 displays the histograms and box and whisker plots for Rats 1, 2, and 3. In Fig 8B, the non-oscillatory controls and oscillatory periods of Rat 1 do not appear to be very different; coherence values between these two periods show to be relatively the same. For Rat 2 and 3 however, the box and whisker plots demonstrate higher coherence values for oscillatory periods, with the greatest difference and highest coherence values occurring in Rat 3. Using the Kruskal-Wallis non-parametric ANOVA test, the mean coherence of oscillatory periods was statistically higher than non-oscillatory periods for Rat 2 and 3, [Rat 2, $H(1, N= 7759) = 114.0788$; Rat 3, $H(1, N=10585) = 1657.32$]. For Rat 1 however, this analysis revealed no significant difference in coherence between oscillatory and non-oscillatory periods, with coherence values that averaged around 0.5.

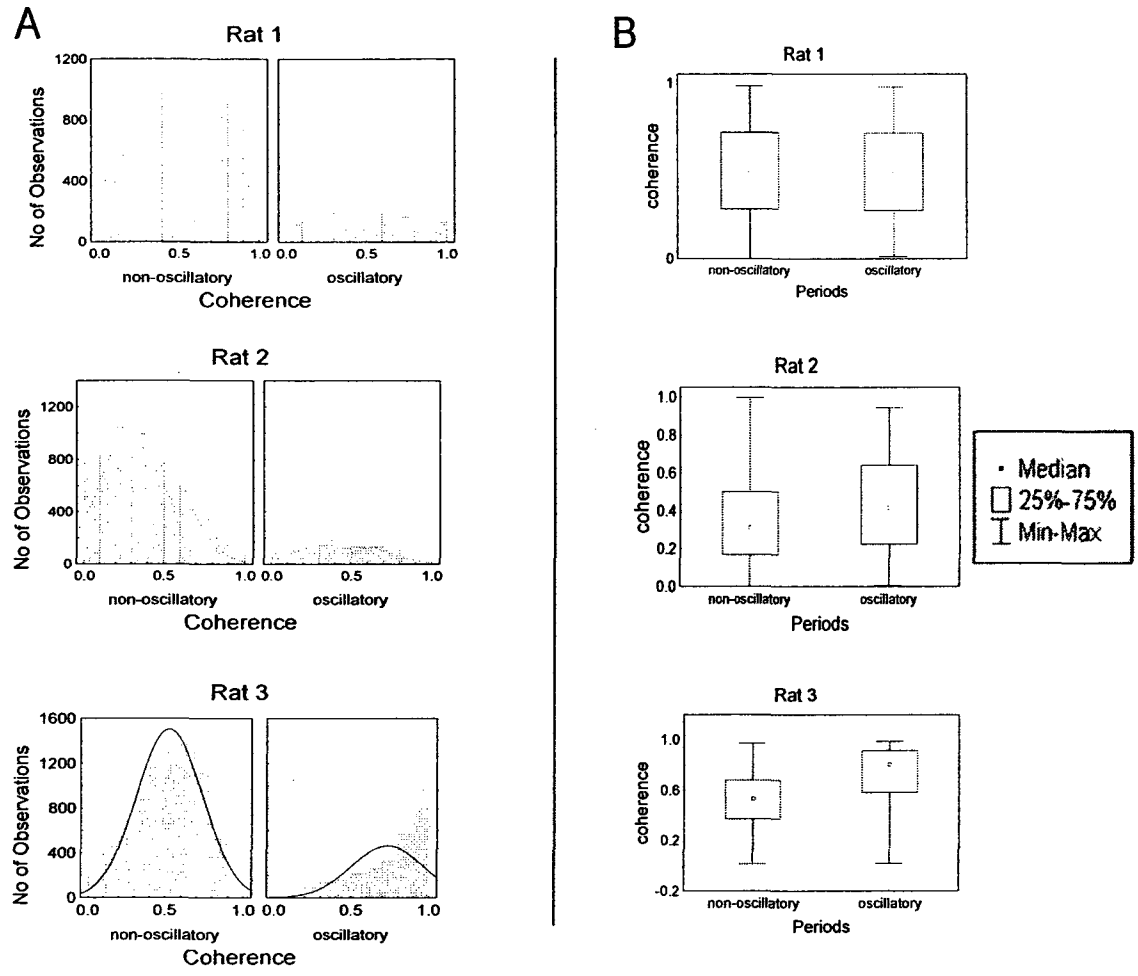

Figure 9. Coherence during non-oscillatory and oscillatory periods for each rat. A: Histogram comparing the distribution of the mean coherence of non-oscillatory and oscillatory periods for Rat 1, 2, 3. B: Box whisker plot analysis of coherence for non-oscillatory and oscillatory periods for Rat 1, 2, 3. For Rat 1, non-oscillatory (0.486) and oscillatory (0.486) periods had no significant difference, $p > 0.05$. For Rat 2, the difference was significant at, $p < 0.05$ for non-oscillatory (0.311) and oscillatory (0.417) periods. Rat 3 was also significant $p < 0.05$, for 05 for non-oscillatory (0.539) and oscillatory (0.809630) periods.

5.4 Oscillations and Coherence at Certain Orientations

The electrode arrangement of each recording site varied across subjects. Fig.10 displays two different orientations for Rat 1; diagonal and 'same needle'. Rat 1 was the only rat to possess a diagonal orientation. The coherence values for this orientation were low, and were similar between periods. In fact, the diagonal orientation had no significant difference between non-oscillatory controls and oscillatory periods H (1, N =6937) =0.2167992. The 'same needle' orientation for Rat 1 however had much higher coherence values for both controls and oscillatory periods; what is interesting is that the controls were more coherent than the oscillatory periods. This was an unusual but statistically significant finding H (1, N = 3824) = 94.37653.

Fig.11 displays the orientation of Rat 2; 'same needle' and coronal. Electrodes arranged in the 'same needle' orientation for Rat 2 have low coherence values across periods, however the oscillatory periods are higher and significantly different from the non-oscillatory controls H (1, N = 2586) = 12.29017. For the coronal orientation of Rat 2, coherence values were higher compared to 'same needle' values. Between control periods and oscillatory periods of the coronal orientation, oscillatory period values were greater and significantly different from the non-oscillatory controls, H (1, N = 5173) = 112.8485.

Rat 3 only had one orientation, 'same needle'. Fig. 12 illustrates in a histogram (A) and box and whisker plot (B) the difference between non-oscillatory controls and oscillatory periods for Rat 3. Coherence values were extremely high for oscillatory

periods, the highest across all rats. The difference between the non-oscillatory controls and the oscillatory periods for Rat 3 is significant, $H(1, N=10585) = 1657.32$. While some orientations displayed greater coherence values than others, our results suggest that electrode orientation plays a large role in the synchrony patterns of LFP oscillations. Orientation had a significant affect in the coronal arrangement for Rat 2, as did 'same needle' for Rat 1, 2, and 3. However the diagonal arrangement in Rat 1 was the only orientation that had no significant difference.

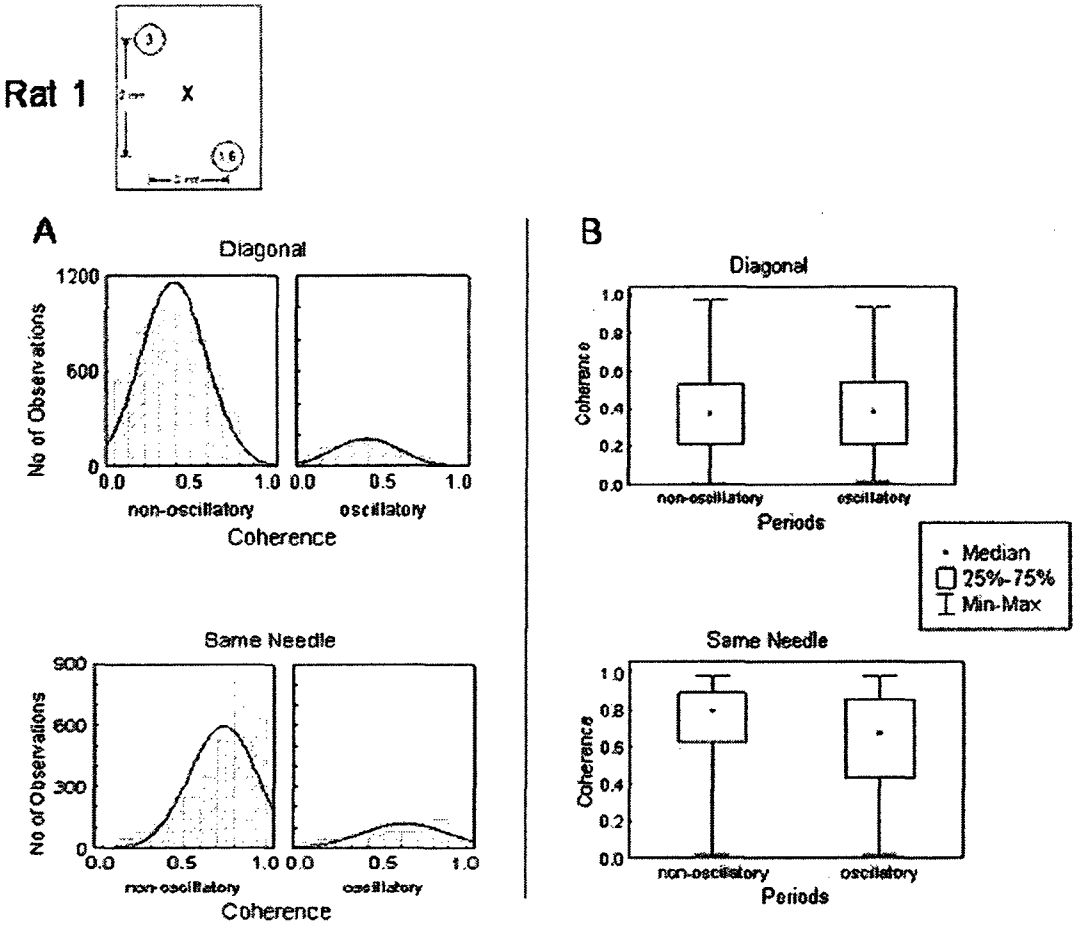

Figure 10. Coherence versus Orientation for Rat 1 during non-oscillatory and oscillatory periods. Top left corner is a electrode arrangement map for Rat 1. A: Histogram comparing the distribution of the mean coherence of non-oscillatory and oscillatory periods for electrodes arranged in diagonal and 'same needle' orientation. B: Box whisker plot of coherence for non-oscillatory and oscillatory periods for diagonal and 'same needle' orientation. In the diagonal arrangement, non-oscillatory (0.373) and oscillatory (0.380) periods were not significant, $p > 0.05$. However, in the "same needle' arrangement, non-oscillatory periods (0.791) were statistically different from oscillatory periods (0.671), $p < 0.05$. This analysis was performed using the Kruskal-Wallis non-parametric ANOVA test.

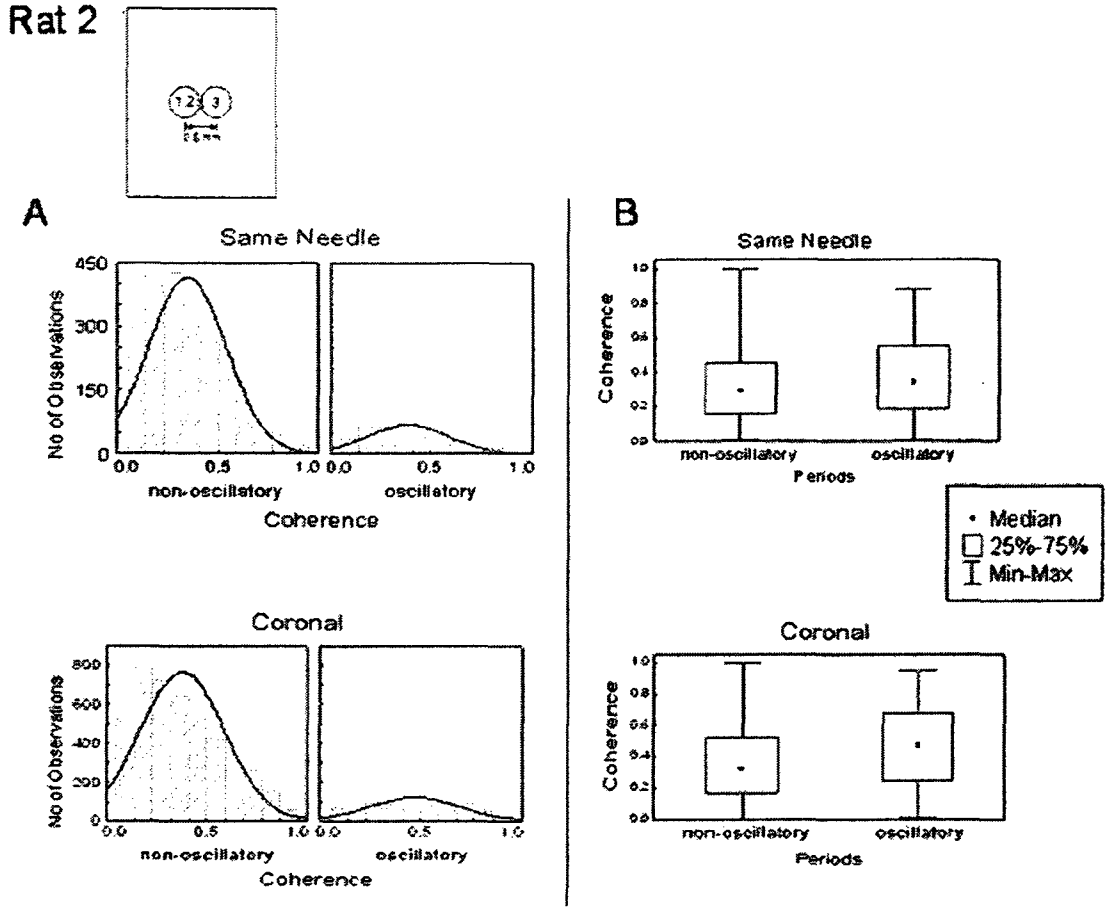

Figure 11. Mean Coherence versus Orientation for Rat 2 during non-oscillatory and oscillatory periods. Top left corner is a electrode arrangement map for Rat 2. A: Histogram comparing the distribution of the mean coherence of non-oscillatory and oscillatory periods for electrodes arranged in the coronal and 'same needle' orientation. B: Box whisker plot analysis of coherence for non-oscillatory and oscillatory periods for coronal and 'same needle' orientation. In the coronal arrangement, non-oscillatory (0.326) and oscillatory (0.380) periods were not significant, $p > 0.05$. In the "same needle' arrangement, non-oscillatory periods (0.290) were statistically different from oscillatory periods (0.339), $p < 0.05$. This analysis was performed using the Kruskal-Wallis non-parametric ANOVA test.

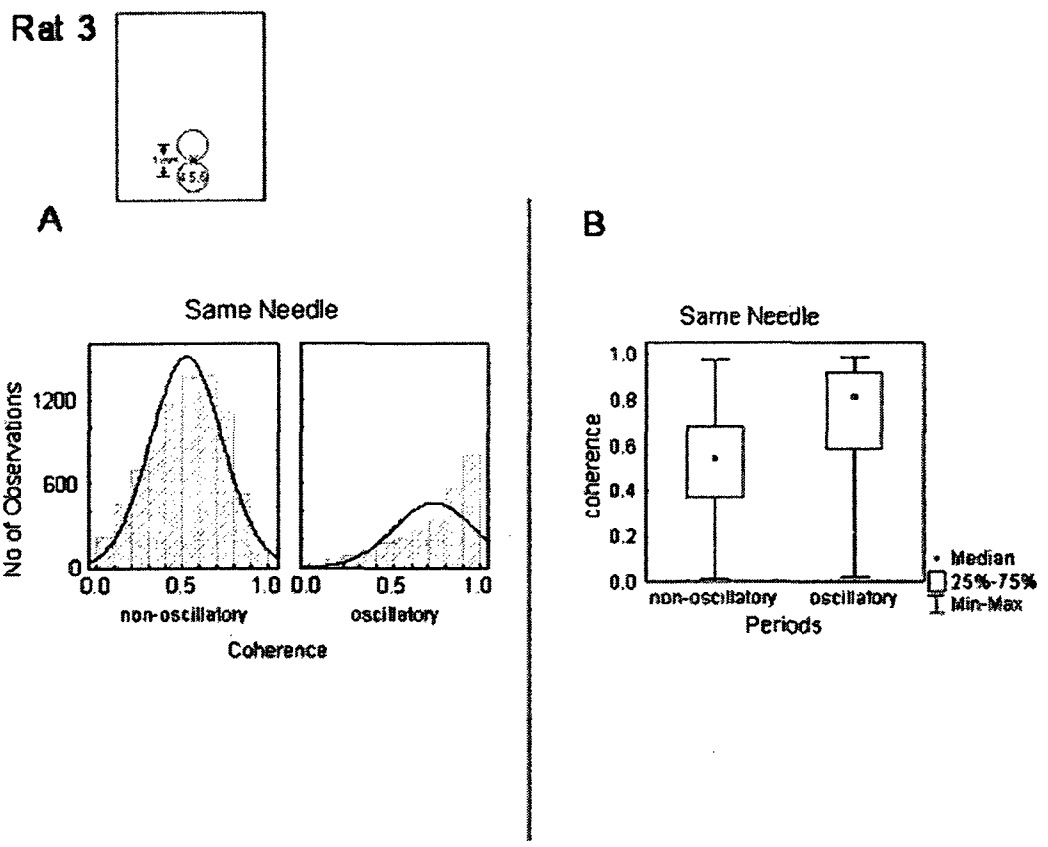

Figure 12. Coherence versus Orientation for Rat 3 during non-oscillatory and oscillatory periods. Top left corner is an electrode arrangement map for Rat 3. A: Histogram comparing the distribution of the mean coherence of non-oscillatory and oscillatory periods for electrodes arranged in the 'same needle' orientation. B: Box whisker plot analysis of coherence for non-oscillatory and oscillatory periods for 'same needle' orientation. In this arrangement, non-oscillatory (0.539) and oscillatory (0.809) periods were significant, $p < 0.05$. This analysis was performed using the Kruskal-Wallis non-parametric ANOVA test.

5.5 Does the electrode used for detecting oscillations influence coherence?

For each rat, oscillations were detected on 1 of 3 electrodes. Electrode channel for detection was based on its location and its capacity to record granule cell layer oscillations; this would yield the highest number of detectable oscillations per channel, and be representative of the GCL influence. A comparison between detected and non-detected electrodes served a purpose of identifying oscillatory recording sites more influenced by the GCL oscillations. For Rat 1, the detected electrode changed for every session, whereas for Rats 2 and 3, the same electrode was detected across sessions. Fig. 13 illustrates the coherence histogram (A) and box and whisker plot (B) for detected and non-detected electrodes of Rat 1. For Rat 1 the detected electrodes [H (1, N = 7168) =21.08060] appear to have significantly more of coherent oscillatory periods then non-oscillatory; however the non-detected electrodes [H (1, N = 3593) = 46.72936)] do not. This finding was unique to Rat 1. The effect of detected and non-detected electrodes on coherence of Rat 2 is illustrated in Fig. 14. Both detected and non-detected electrodes had a significant difference between oscillatory and non oscillatory control periods for Rat 2 [detected, H (1, N =5173) =112.8485); non-detected, H (1, N = 2586) = 12.29017)]. The same results can be seen for Rat 3 in Fig. 15; [detected, H (1, N = 7061) = 1118.637); non-detected, H (1, N = 3524) = 538.8560). Therefore, electrode comparisons that shared a detected electrode had significantly higher mean coherence than non-detected electrode comparisons. Oscillatory activity is improved by the detected electrode.

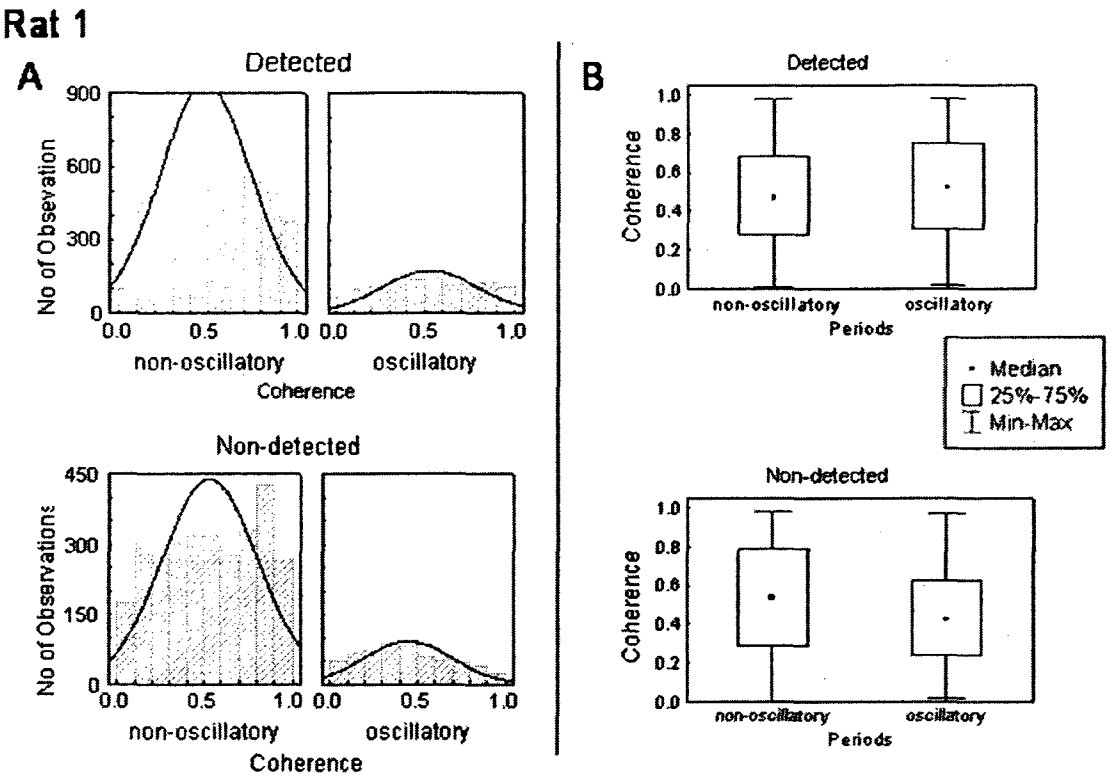

Figure 13. Coherence of detected electrodes versus non-detected electrodes for Rat 1 during non-oscillatory and oscillatory periods. A: Histogram comparing the distribution of the mean coherence of non-oscillatory and oscillatory periods for electrodes that were either detected or paired with a detected electrode ('detected'), and those that were not ('non-detected'). B: Box whisker plot analysis of coherence for non-oscillatory and oscillatory periods for 'detected' and 'non-detected' electrodes. For 'detected' electrodes, non-oscillatory periods (0.468) had less coherence than oscillatory periods (0.518), and this difference was significant, $p < 0.05$. For 'non-detected' electrodes, non-oscillatory periods (0.534) were more coherent than oscillatory (0.410), and this difference was also significant, $p < 0.05$. These analyses were performed using the Kruskal-Wallis non-parametric ANOVA test.

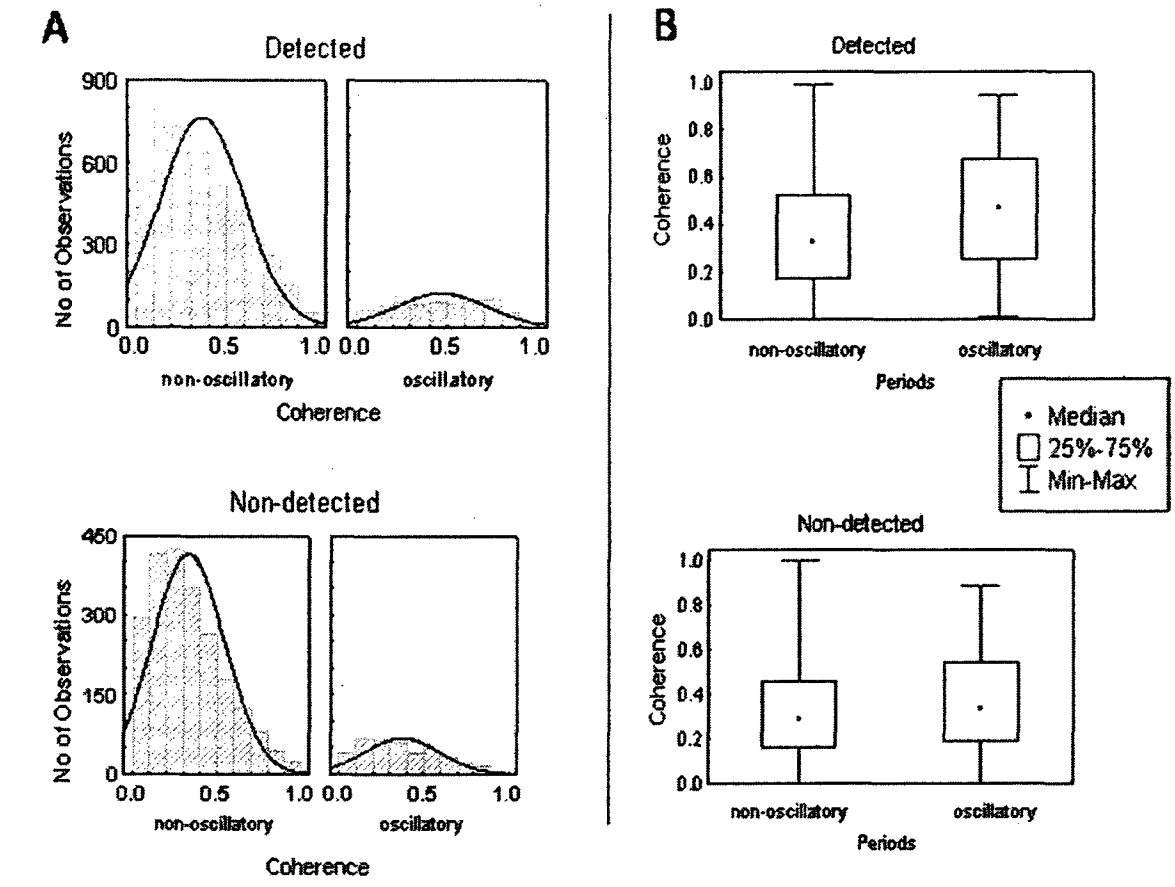

Figure 14. Coherence of detected electrodes versus non-detected electrodes for Rat 2 during non-oscillatory and oscillatory periods. A: Histogram comparing the distribution of the mean coherence of non-oscillatory and oscillatory periods for electrodes that were either detected or paired with a detected electrode ('detected'), and those that were not ('non-detected'). B: Box whisker plot analysis of coherence for non-oscillatory and oscillatory periods for 'detected' and 'non-detected' electrodes. For 'detected' electrodes, non-oscillatory periods (0.326) had less coherence than oscillatory periods (0.470), and this difference was significant, $p < 0.05$. For 'non-detected' electrodes, non-oscillatory periods(0.290) were less coherent than oscillatory (0.389), this difference was also significant, $p < 0.05$. These analyses were performed using the Kruskal-Wallis non-parametric ANOVA test.

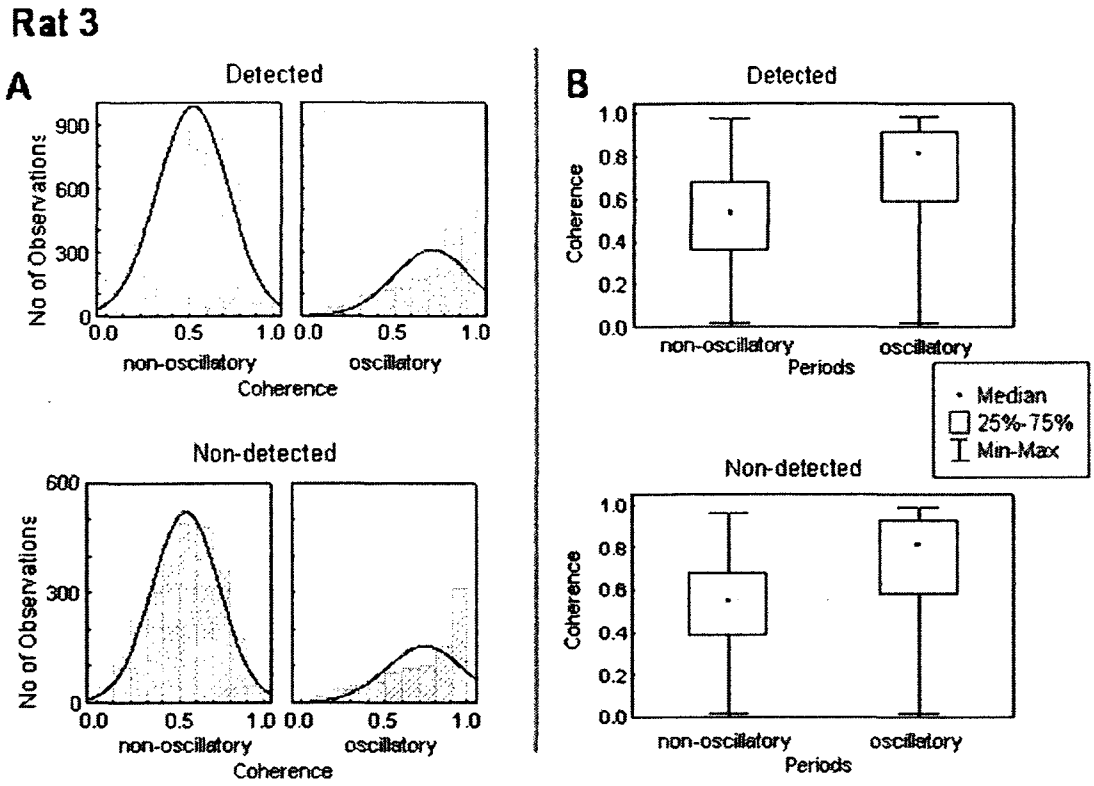

Figure 15. Coherence of detected electrodes versus non-detected electrodes for Rat 3 during non-oscillatory and oscillatory periods. A: Histogram comparing the distribution of the mean coherence of non-oscillatory and oscillatory periods for electrodes that were either detected or paired with a detected electrode ('detected'), and those that were not ('non-detected'). B: Box whisker plot analysis of coherence for non-oscillatory and oscillatory periods for 'detected' and 'non-detected' electrodes. For 'detected' electrodes, non-oscillatory periods (0.535) had less coherence than oscillatory periods (0.808), and this difference was significant, $p < 0.05$. For 'non-detected' electrodes, non-oscillatory periods (0.547) were less coherent than oscillatory (0.811), this difference was also significant, $p < 0.05$. These analyses were performed using the Kruskal-Wallis non-parametric ANOVA test.

CHAPTER 6:

DISCUSSION

Our results show that oscillations that occur within a frequency range of 6-11 Hz in the GCL influence synchrony among multiple simultaneous LFPs recorded in the cerebellar cortex *in vivo*. Coherence between electrodes was significantly stronger during periods where oscillations were present, contrary to control periods that had no oscillations. Our results have important implications for network activity organization in the cerebellar cortex of the awake rat: showing that oscillatory activity starting in the GCL can shape population patterns in the animal at rest.

Hartmann and Bower (1998) also identified synchrony of cerebellar cortex GCL LFPs; they found certain examples of synchrony on wire electrodes near and far. From their results, however, the importance of synchrony observed between cerebellar hemispheres overshadowed local organization. What is telling from our results is that synchrony was detected between LFPs organized in varying spatial arrangements providing a greater nuance in the local network-shaping capacities of GCL activity.

It was important to assess whether electrodes used for detecting oscillations had an influence on GCL LFP coherence. After analyzing 'detected' and 'non-detected' channels, we came to the conclusion that the detected electrode actually improved the coherence between channels. This implies that while LFPs from all electrodes could be compared, the GCL-specific coherence comparisons, involving the oscillatory detections,

improved the oscillatory coherence: the purer GCL influence could better trigger coherence.

6.0 Coherence across rats

Across rats, oscillatory periods had significantly greater coherence than non-oscillatory periods; however this was not the case for Rat 1 (Fig. 9), where no significant difference occurred. The inconsistency in results for Rat 1 did not occur because of a lack LFP synchrony, in fact coherence levels for particular site comparisons for Rat 1 reached over 0.8 depending on the session (Table 2). A few reasons could have changed the results: (1) As shown, when considering the detected channel, the coherence was better for oscillatory periods: the detected channel was more a factor in this case, so that pooling all comparisons could have a weakening effect; (2) another factor which may have occurred is a discrepancy in the number of oscillatory periods detected compared to non-oscillatory periods. Across rats there were more oscillatory periods detected compared to non-oscillatory periods, however Rat 1 has the greatest difference compared to Rat 2 and 3 (Table 1). This potentially may have skewed the results, in the event that truly oscillatory periods were overlooked as non-oscillatory periods. For example, LFP within the 6 -11 Hz range that did not last a time window of 1 second would have been detected as non-oscillatory and contributed to its high coherence values. Perhaps a better indicator, than rat comparison, of how oscillations influence the synchrony between LFPs would be a look at how the GCL LFPs are organized. This was done by comparing recording sites that were organized in a coronal, diagonal (coronal + sagittal) and 'same needle' arrangement.

6.1 Coherence and Orientation

The arrangement of the recording electrodes played a major role in the influence of oscillations on LFP synchrony. Electrodes that shared a common needle, with regards to the structure of the headstage, showed the greatest synchrony among GCL LFPs. This is true for all three rats, who share a 'same needle' orientation. For Rat 3, the only electrode arrangement recorded was 'same needle', while Rat 2 also had electrodes recorded in the coronal arrangement. In these rats, oscillatory periods of 'same needle' orientation had the highest levels of coherence compared to diagonal and coronal orientations. Coherence levels were particularly high for Rat 3, whose quartile values for oscillatory periods did not drop below 0.6 (Figure 8). For this rat, all three electrodes must have been in the GCL of the cerebellum. Electrodes in the 'same needle' arrangement naturally were more proximal, compared to those in the coronal or diagonal arrangement, however the recording sites of these in this arrangement had a depth range that varied as much as the other orientations, and therefore coherence found in this arrangement can not be due to different electrodes recording the same signal of the same GCL.

For Rat 1 the greatest coherence was also found in the 'same needle' orientation, and this in fact was the only orientation for Rat 1 that was significant at all; however, greater synchrony was found in non-oscillatory control periods compared to oscillatory periods. Oscillations recorded in the diagonal orientation in Rat 1 had a greater tendency

to synchronize than the non-oscillatory control LFPs; however this difference was not significant. The implications of this will be discussed shortly.

As mentioned above, the electrodes recorded in Rat 2 had a coronal orientation. This arrangement had oscillatory GCL LFPs that were significantly more coherent than non-oscillatory controls. What is interesting is that coronal orientation had an effect on LFP coherence, but the diagonal orientation did not. These results implicate a synchronization of the cerebellar GCL LFPs that could implicate coronal connections. Mossy fibers carry afference from cortical areas and bring it to the GCL of the cerebellar cortex where they excite granule cells. These granule cells excite parallel fibers which synapse onto Purkinje cells, but also Golgi cells. The perpendicular arrangement between parallel fibers, Golgi cells, and Purkinje cells is ideal for dispersing input into a large synaptic space for refined computation (Buzsaki, 2006). Golgi cells prevent too much parallel fiber activation by inhibiting granule cells (Palay and Chan-Palay, 1974). This Golgi cell feedback inhibition creates oscillations in the GCL at a rate of 10-50 Hz (Maex and DeSchutter, 1998). The frequency of these oscillations is due to the conduction speed and length of the parallel fibers (Maex and DeSchutter, 2005). Therefore, our results suggest that coherence could be better coronally because of the connections via parallel fibers. Having such an organization would permit areas of greater distances (up to 5-7 mm long – the average length of a parallel fiber) to be synchronized as well.

Welsh and colleagues (1995), in rats, found complex spike rhythmicity in the same frequency range of membrane potential oscillations of the inferior olive (10 Hz).

These patterns of synchronous olivocerebellar activity expanded across parasagittal bands during movement. Similar findings by Lang et al. (1999), who studied spontaneous complex spike activity in awake rats that were immobile, revealed synchrony between spikes in both the sagittal and coronal orientation. While synchrony displayed a rostrocaudal preference, the degree of synchronous activity mediolaterally traveled up to 500 μm. Interestingly, simple spikes are modulated by complex spike synchrony (Schwarz and Welsh, 2001). This relationship is not due to direct interaction of climbing and mossy fiber systems but rather mediated by cerebellar networks. Schwarz and Welsh (2001) suggest that complex spikes that synchronize mediolaterally could extend effects to simple spikes via a Lugaro cell network. Lugaro cells are inhibitory neurons that project along the transverse axis and synapse onto Golgi cells (Dieudonne and Dumoulin, 2000). These cells may form a circuit where climbing fiber collaterals could modulate Golgi cells that expand into the mediolateral plane. This Lugaro-Golgi cell network may contribute to the coronal synchrony observed in the LFPs of the GCL.

We must point out, however, that we did not have the chance in this thesis to investigate all possible orientations: what is missing is a true distinction in the sagittal plane to make a full comparison. However, we have managed to identify certain trends in the data, based on the connectivity in diagonal vs. coronal organizations. Other recordings and more analyses will be necessary to contrast additional orientations.

An important result we found is the effect of oscillations on the network coherence. Golgi cells control information flow in the GCL of the cerebellum (Eccles,

1967). Since the GCL can oscillate at certain frequencies during rest and cease with movement, Golgi cells must influence this network activity pattern. The Golgi cells control the rhythmicity of the LFPs, and cerebellar networks are what synchronize them. It is unclear why the cerebellum may benefit from such synchrony in the GCL; however, knowing how this network activity pattern functions is integral to understanding the cerebellum as a rhythm generator.

6.2 Significance and Future Directions

Oscillations reflect synchronous activity in a population of neurons. The function of these oscillations may be to serve as a binding mechanism for information processing. This study suggests that oscillations influence the coherence between LFPs that run along the transverse axis of the cerebellar cortex, suggesting a compartmentalization to this synchrony. The granular layer of the cerebellum is also highly compartmentalized (Ozol and Hawkes, 1997). Afferent somatosensory projections to this layer are a major contributor to the compartmentalization. Granule cells that align perpendicular to the axis of the folia form columns of somatotopically coherent input in crus I, II, and the paramedian lobule (Shambes et al. 1978). The term 'patch' is used to refer the basic column-like assemblies of the peripheral projections and the overall patches make up mosaics that represent different regions of the periphery. This arrangement suggests that the cerebellar computations involve non-local interactions among the tactile inputs (Nelson and Bower, 1990). The long extensions of the parallel fibers are what are binding these patches, allowing information processing to occur in the cerebellar cortex.

Binding can occur at a systems level or within a local circuit. Oscillations can facilitate this mechanism by synchronizing neural activity. The Demonstration of synchronous activity at the population level in the GCL of the awake rat indicates organized network activity. If oscillations facilitate this synchrony, then they could serve a functional purpose. It is possible that oscillations may code information in the climbing fiber and mossy fiber systems. To investigate this further, it would be valuable to probe the interaction of complex and simple spikes and relate this firing with LFP activity across all the layers of the cerebellar cortex and examine the differences among cerebellar population patterns.

REFERENCES:

Braitenberg V (1967) Is the cerebellar cortex a biological clock in the millisecond range? Prog.Brain Res. 25: 334-346

Braitenberg V, Heck D, Sultan F (1997) The detection and generation of sequences as a key to cerebellar function: experiments and theory. Behav.Brain Sci. 20: 229-245

Buzsaki G (2006) Rhythms of the Brain. New York: Oxford University Press

Courtemanche R (1999) Oscillations Locales dans le cervelet organization, modulation et synchronization avec le cortex cerebral lors dur mouvment. PhD Thesis. University of Montreal.

Courtemanche R, Lamarre Y (2005) Local field potential oscillations in primate cerebellar cortex: synchronization with cerebral cortex during active and passive expectancy. J.Neurophysiol. 93: 2039-2052

de Solages C, Szapiro G, Brunel N, Hakim V, Isope P, Buisseret P, Rousseau C, Barbour B, Lena C (2008) High-frequency organization and synchrony of activity in the purkinje cell layer of the cerebellum. Neuron 58: 775-788

De Zeeuw CI, Hoebeek FE, Schonewille M (2008) Causes and consequences of oscillations in the cerebellar cortex. Neuron 58: 655-658

Dieudonne S, Dumoulin A (2000) Serotonin-driven long-range inhibitory connections in the cerebellar cortex. J.Neurosci. 20: 1837-184

Eccles JC (1967) Circuits in the cerebellar control of movement. Proc.Natl.Acad.Sci.U.S.A 58: 336-343

Edge AL, Marple-Horvat, DE, Apps R (2003) Lateral cerebellum, functional localization within crus I and correspondence to cortical zones. Eur.J.Neurosci. 18: 1468-1485

Gray CM (1994) Synchronous oscillations in neuronal systems: mechanisms and functions. J.Comput.Neurosci. 1: 11-38

Hartmann MJ, Bower JM AL, Marple-Horvat DE, Apps R (2003) Lateral cerebellum: functional (1998) Oscillatory activity in the cerebellar hemispheres of unrestrained rats. J.Neurophysiol. 80: 1598-1604

Hartmann MJ, Bower JM (2001) Tactile responses in the granule cell layer of cerebellar folium crus IIa of freely behaving rats. J.Neurosci. 21: 3549-3563

Heck D (1999) Sequential stimulation of rat and guinea pig cerebellar granular cells in vitro leads to increasing population activity in parallel fibers. Neurosci.Lett. 263: 137-140

Heck D, Sultan F (2002) Cerebellar structure and function: making sense of parallel fibers. Hum.Mov Sci. 21: 411-421

Heck DH, Thach WT, Keating JG (2007) On-beam synchrony in the cerebellum as the mechanism for the timing and coordination of movement. Proc.Natl.Acad.Sci.U.S.A 104: 7658-7663

Ito M (1984) The cerebellum and neural control. New York: Raven Press

Keating JG, Thach WT (1995) Nonclock behavior of inferior olive neurons: interspike interval of Purkinje cell complex spike discharge in the awake behaving monkey is random. J.Neurophysiol. 73: 1329-1340

Lang EJ, Sugihara I, Welsh JP, Llinas R (1999) Patterns of spontaneous purkinje cell complex spike activity in the awake rat. J.Neurosci. 19: 2728-2739

Llinas RR, Walton KD, Lang EJ (1990) Cerebellum. In G.M Shepherd (Ed), The synaptic organization of the brain. issues (271-309). London: Oxford University Press.

MacKay, W (1998) Synchronized neuronal oscillations and their role in motor processes. Trends Cog. Sci. 5: 176-182

Maex R, De Schutter E (1998) Synchronization of golgi and granule cell firing in a detailed network model of the cerebellar granule cell layer. J.Neurophysiol. 80: 2521-2537

Maex R, De Schutter E (2005) Oscillations in the cerebellar cortex: a prediction of their frequency bands. Prog.Brain Res. 148: 181-188

Middleton SJ, Racca C, Cunningham MO, Traub RD, Monyer H, Knopfel T, Schofield IS, Jenkins A, Whittington MA (2008) High-frequency network oscillations in cerebellar cortex. Neuron 58: 763-774

Nelson ME, Bower JM (1990) Brain maps and parallel computers Trends Neurosci. 13: 403-408

O'Connor SM, Berg RW, Kleinfeld D (2002) Coherent electrical activity between vibrissa sensory areas of cerebellum and neocortex is enhanced during free whisking. J.Neurophysiol. 87: 2137-2148

Ozol KO, Hawkes R (1997) Compartmentation of the granular layer of the cerebellum. Histol.Histopathol. 12: 171-184

Palay SM, Chan-Palay V (1974) Cerebellar Cortex: Cytology and Organization. New York: Springer-Verlag.

Paxinos G, Watson C (1986) The rat brain in stereotaxic coordinates. New York: Academic Press

Pellerin JP, Lamarre Y (1997) Local field potential oscillations in primate cerebellar cortex during voluntary movement. J.Neurophysiol. 78: 3502-3507

Schwarz C, Welsh JP (2001) Dynamic modulation of mossy fiber system throughput by inferior olive synchrony: a multielectrode study of cerebellar cortex activated by motor cortex. J.Neurophysiol. 86: 2489-2504

Shambes GM, Gibson JM, Welker W (1978) Fractured somatotopy in granule cell tactile areas of rat cerebellar hemispheres revealed by micromapping
Brain Behav.Evol. 15: 94-140

Shin SL, De Schutter E (2006) Dynamic synchronization of Purkinje cell simple spikes. J.Neurophysiol. 96: 3485-3491

Uhlhaas PJ, Haenschel C, Nikolic D, Singer W (2008) The role of oscillations and synchrony in cortical networks and their putative relevance for the pathophysiology of schizophrenia. Schizophr.Bull. 34: 927-943

Volny-Luraghi A, Maex R, Vosdagger B, De Schutter E (2002) Peripheral stimuli excite coronal beams of Golgi cells in rat cerebellar cortex. Neuroscience 113: 363-373

Vos BP, Maex R, Volny-Luraghi A, De Schutter E (1999) Parallel fibers synchronize spontaneous activity in cerebellar Golgi cells. J.Neurosci. 19: RC6

Welsh JP, Lang EJ, Suglhara I, Llinas R (1995) Dynamic organization of motor control within the olivocerebellar system. Nature 374: 453-457

Whittington MA, Traub RD, Jefferys JG (1995) Synchronized oscillations in interneuron networks driven by metabotropic glutamate receptor activation. Nature 373: 612-615

Yarom Y, Cohen D (2002) The olivocerebellar system as a generator of temporal patterns. Ann.N.Y.Acad.Sci. 978: 122-134